Journal of King Saud University – Engineering Sciences (2015) **27**, 43–48

King Saud University

Journal of King Saud University – Engineering Sciences

www.ksu.edu.sa
www.sciencedirect.com

ORIGINAL ARTICLE

Morphology study of electrodeposited zinc from zinc sulfate solutions as anode for zinc-air and zinc-carbon batteries

Nurhaswani Alias, Ahmad Azmin Mohamad *

School of Materials and Mineral Resources Engineering, Universiti Sains Malaysia, 14300 Nibong Tebal, Penang, Malaysia

Received 21 February 2013; accepted 12 March 2013
Available online 26 March 2013

KEYWORDS

Zn deposition;
Copper substrate;
Current density;
Zinc-air battery;
Zinc-carbon battery

Abstract The morphology of Zinc (Zn) deposits was investigated as anode for aqueous batteries. The Zn was deposited from zinc sulfate solution in direct current conditions on a copper surface at different current densities. The morphology characterization of Zn deposits was performed via field emission scanning electron microscopy. The Zn deposits transformed from a dense and compact structure to dendritic form with increasing current density. The electrodeposition of Zn with a current density of 0.02 A cm^{-2} exhibited good morphology with a high charge efficiency that reached up to 95.2%. The Zn deposits were applied as the anode in zinc–air and zinc–carbon batteries, which gave specific discharge capacities of 460 and 300 mA h g^{-1}, respectively.

1. Introduction

Zinc (Zn) is a promising anode candidate for secondary alkaline batteries because of its abundance, relatively low cost, compatibility with aqueous electrolytes, and low-toxic element (Hilder et al., 2012). In secondary alkaline batteries, the anode should be efficient as a reducing agent and must have a high coulombic output, good conductivity, ease of fabrication, and low cost (Linden, 2001). The applications of Zn as an anode tremendously increased because Zn possesses these favorable properties. Furthermore, Zn has a large overpotential for hydrogen gas evolution, which allows Zn to operate at lower potentials than the window stability of water (Abe and Miyazaki, 2012). A Zn anode is generally fabricated by various methods such as electrodeposition (Gomes and da Silva Pereira, 2006; Popov et al., 1978) and paste drying (Masri and Mohamad, 2009).

Recent investigations have highlighted electrodeposition as an attractive approach that not only provides a cost-effective intensive method that does not require any equipment, but also has the advantage to control the shape and grain size of the deposit and can provide a high surface area (Bunshah, 1994; Leung et al., 2011; Lehr and Saidman, 2012). Bicelli et al. (2008) also reported that interdiffusion or chemical reactions can be minimized using a low processing temperature (room temperature) during the electrodeposition process.

* Corresponding author. Tel.: +60 4599 6118; fax: +60 4594 1011.
E-mail address: azmin@eng.usm.my (A.A. Mohamad).

Peer review under responsibility of King Saud University.

ELSEVIER Production and hosting by Elsevier

http://dx.doi.org/10.1016/j.jksues.2013.03.003

Therefore, various studies on the electrodeposition of Zn were performed in different operating conditions to improve the morphology and properties of metal deposits, which depend on the application of the material.

The peak current density is a critical factor which results in refining of the Zn deposits' grain without the formation of dendrites (Shaigan et al., 2010). According to Leung et al. (2011), a high current efficiency of Zn deposits at a low current density (0.02 A cm^{-2}) in methanesulfonic acid electrolyte was obtained without the presence of additives. The work by Freitas and de Pietre (2005) also found that the current density not only affects the deposit morphology, but also the current efficiency. Although Zn electrodeposition has been performed for a long time, only a few systematic studies were carried out on Zn deposits in aqueous battery applications (Shaigan et al., 2010; Abe and Miyazaki, 2012). Thus, a preliminary study that focuses on the use of electrodeposited Zn as an anode for aqueous battery applications need to be conducted to determine the optimum properties of the anode as well as to improve the battery performance.

In this study, the electrodeposition process was measured on the deposition of Zn on a copper (Cu) plate surface using direct current conditions. Different current densities were applied in a Zn sulfate ($ZnSO_4$) solution without the presence of additives. The morphology analysis was performed to investigate the correlation between the morphology of the sample and the current density. Moreover, phase characterization analysis was carried out to support the findings. The Zn deposit was used as the anode material in zinc–air (Zn–air) and zinc–carbon (Zn–carbon) batteries. Finally, the electrochemical performance of Zn–air and Zn–carbon batteries, where Zn deposits were used as anodes, was evaluated.

2. Experimental

2.1. Electrodeposition of zinc

The electrodeposition of Zn on a Cu plate was carried out in a two-electrode system. The Cu plate (1×5 cm^2) was used as the substrate. Meanwhile, a high purity Zn plate (99.98%, Alfa Aesar) with a dimension of 2×4 cm^2 was used as the anode. The surface of both plates was polished using a common metallographic technique, followed by sonication in acetone for 10 min. The electrodes were then rinsed with deionized water and dried at room temperature. Moreover, 1 M $ZnSO_4$ solution was prepared as an electrolyte by dissolving analytical grade $ZnSO_4 \cdot 7H_2O$ (16.14 g, Univar) in 250 cm^3 of deionized water.

Electrodeposition was performed using an electrochemical cell, as schematically shown in Fig. 1a. The deposit area was fixed at 1 cm^2 with a 1 cm gap between the Zn and Cu plate. The volume of electrolyte contained in the system was 25 cm^3, and the electrodeposition process was carried out in a 50 cm^3 glass beaker. Zn electrodeposits were prepared by applying a direct current at 0.01, 0.02, 0.04, 0.06, 0.08, and 0.10 A cm^{-2} for 1 h. All electrodeposition experiments were carried out at ambient temperature. After the deposition, the samples were rinsed with acetone and deionized water before drying at room temperature.

The weight of the Zn deposits was calculated by weighing the samples before and after the deposition process. The current efficiency of the electrodeposition was then calculated from the weight ratio of the Zn deposits to the theoretically expected weight of Zn deposits, which is based on the amount of current used according to Faraday's laws of electrolysis (Linden, 2001):

$$M = \frac{QM}{nF} \tag{1}$$

where m is the mass of the deposits, F is the Faraday constant (96,500 C mol^{-1}), Q is the electric charge passed, M is the molar mass of the species, and n is the electrical charge involved in the reaction.

Field emission scanning electron microscopy (FESEM, Zeiss Supra™, 35VP) was performed to characterize the morphologies of the Zn electrodeposits. X-ray diffraction (XRD, Bruker AXS D9) was also performed on the optimum Zn deposit sample to identify the purity of the sample.

2.2. Zinc–air and zinc–carbon battery assembly

Fig. 1b and c shows the schematic design of the discharge characterization of Zn deposits in Zn–air and Zn–carbon batteries, respectively. The poly(methyl-methacrylate) casing used for the Zn–air battery was similar to that of a previous report (Koh et al., 2011). The air–cathode (Meet, Korea) with an active area of 12.5 cm^2 was used, and was composed of nickel foam coated with polytetrafluoroethylene (PTFE) and a mixture of MnO_2, carbon, and a PTFE binder. Meanwhile, a commercial carbon rod (Good Fellow, Korea) with a geometric area of 12.6 cm^2 was utilized as a counter electrode in the Zn–carbon battery.

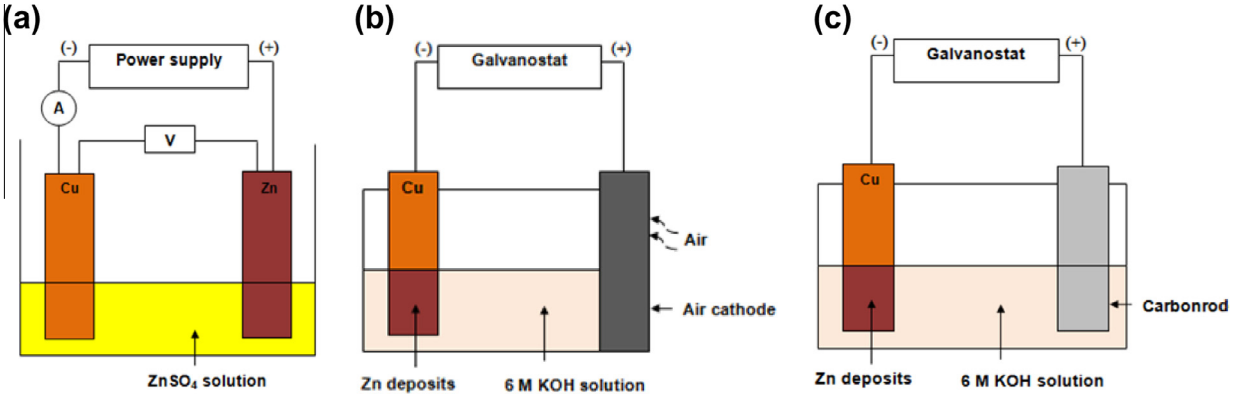

Figure 1 Schematic of (a) Zn electrodeposition on the Cu electrode, and (b) Zn–air and (c) Zn–carbon battery construction.

Both aqueous battery systems used 6 M potassium hydroxide (KOH) with the same volume (25 cm^3) as the electrolyte. The electrochemical measurements for both battery systems were done using a WonATech battery testing unit. The cell was discharged using a constant current of 1 mA at ambient temperature. The generated cell potential was measured over time until the potential dropped to 0.6 V.

3. Results and discussion

3.1. Morphology study of zinc deposits

Fig. 2 shows the morphologies of Zn plate, Cu plate, and Zn deposit at different current densities. Smooth surfaces can be observed for the Zn and Cu plate samples before the electrodeposition process (Fig. 2a and b). At a low current density (0.01 A cm^{-2}), a thin deposited layer of Zn with sparse nucleation was observed on the Cu surface (Fig. 2c). When the current density was increased to 0.02 A cm^{-2}, the morphology changed to a hexagonal-like crystalline structure with a strict layer-by-layer flat platelet structure on the Cu surface (Fig. 2d). However, dense nucleation and irregular growth of metallic Zn were detected when Zn was deposited at current densities >0.04 A cm^{-2} (Fig. 2e and g). Finally, a flake-like structure evolved after electrodeposition was performed at a high current density of 0.10 A cm^{-2} (Fig. 2h). Meanwhile, all electrodeposition samples were fully covered with Zn deposits.

The crystallization process of the Zn deposit generally begins with the growth of nuclei (Freitas and de Pietre, 2005). This growth initiated at a rate proportional to the current passed. When the electrolysis process occurs via direct current, more electrons move toward the negative electrode. Within the electrolytes, the negative electrodes are surrounded with Zn^{2+} and H^+ ions. These ions are adsorbed onto the substrate surface via a weak Van der Waals bond, which allows surface diffusion. This diffusion results in the reduction of ions at more

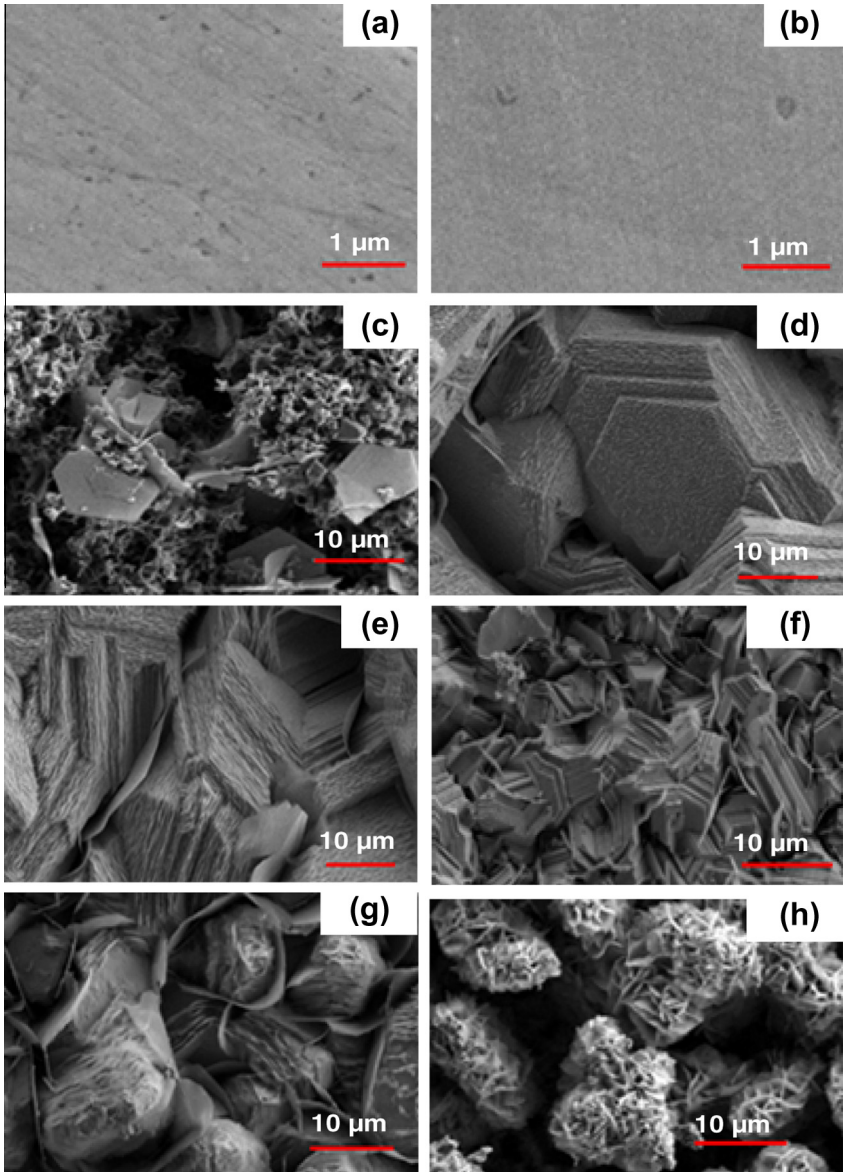

Figure 2 FESEM images of (a) Zn plate, (b) Cu plate, and Zn deposits at current densities of (c) 0.01, (d) 0.02, (e) 0.04, (f) 0.06, (g) 0.08, and (h) 0.10 A cm^{-2}.

favorable sites. The reduction of Zn^{2+} involves gaining two electrons to form zero-valent Zn metal deposits on the Cu plate. A simplified cell reaction can be illustrated as follows:

$$\text{Oxidation process}: \quad Zn \rightarrow Zn^{2+} + 2e^- \tag{2}$$

$$\text{Reduction process}: \quad Zn^{2+} + 2e^- \rightarrow Zn \tag{3}$$

This redox reaction concurrently occurs without changing the original composition of the electrolyte and maintaining the solution more or less uniformly (Lou and Huang, 2006). In fact, the reduction of H^+ to form hydrogen (H_2) gas also competes with the reduction of Zn in an acidic sulfate solution, which follows the Eq. (4):

$$\text{Hydrogen evolution}: \quad 2H^+ + 2e^- \rightarrow H_2 \quad E^\circ = 0.00V \tag{4}$$

The slow electrodeposition process at a current density of 0.01 A cm^{-2} results in a low electron transfer. Therefore, only a few Zn^{2+} were reduced and deposited on the substrate. However, the rate of deposition increased with increasing current density, which results in a large amount of Zn^{2+} being reduced to form a dense and planar structure of the nuclei. The formation of dendrites is enabled at higher current densities when the Zn nuclei start to overlap and agglomerate together to maintain a lower surface energy (Li et al., 2007). The irregular growth of Zn deposits is also accompanied by the evolution and adsorption of hydrogen bubbles, as shown in Eq. (4).

The evolution of Zn deposits at high magnification is shown in Fig. 3. This result is in accordance with those reported by Sharifi et al. (2009), which explained that the change in morphology of Zn powder from dense and uniaxial to disperse and dendritic was due to the increase in current density. Besides that, a similar hexagonal-like crystalline structure was reported by other researchers (Leung et al., 2011; Gomes and da silva Pereira, 2006), which confirmed that this structure is a typical morphology of Zn deposits in the absence of additives. This morphology then changes to a relatively rough and irregular structure with the continued growth and uneven stacking of flat plates at a high current density. Based on the morphology study result, Zn deposition at a current density of 0.02 A cm^{-2} was chosen as the optimum condition for further analyses.

3.2. Structure analysis

Fig. 4 shows the XRD peaks of Cu plate, Zn plate, and Zn deposits at a current density of 0.02 A cm^{-2}. The Cu peaks were detected at $2\theta = 43.46°$, 50.69°, and 74.67°. These peaks correspond to the (1 1 1), (2 0 0), and (2 2 0) planes, respectively, and conform to the main element of the substrate used when the peaks are in agreement with the International Center for Diffraction Data (ICDD) File No. 00-004-0836. The measurement also shows the presence of pure Zn deposits at $2\theta = 43.47°$, which corresponds to the (1 0 1) plane and matches with ICDD File No. 00–004–0831 with several minor peaks at $2\theta = 36.33°$, 39.32°, 54.58°, 70.19°, 82.34°, and 86.90°.

The results reveal that Zn deposited at a current density of 0.02 A cm^{-2} indicates a strong Zn orientation at (1 0 1) plane. However, Chu et al. (1981) explained that the strong diffraction peak around 43° could be attributed to the Cu–Zn brass phase because of the closer gap between the Zn (1 0 1) and Cu (1 1 1) peaks. In this work, no Cu–Zn brass peak was clearly defined because most peaks resemble the individual peaks of Zn and Cu elements. In fact, the high peak intensity of Zn deposits at (1 0 1) plane is similar to the dominant peak of pure Zn. Thus, the results confirm that Zn was deposited on the Cu surface during the electrodeposition process in $ZnSO_4$ solution.

Table 1 shows the efficiency of Zn deposition on the Cu plate at 0.02 A cm^{-2} for 1 h. The electrodeposition process of Zn at a current density of 0.02 A cm^{-2} achieved a high current efficiency of 95.2%. Baik and Fray (2001) explained that the high current efficiency is due to the present preferred texture of the deposit with less defects and grain boundaries so that nucleation sites are available for H_2 gas evolution. On the other hand, the average value of the efficiency is always less than 100% because of side reactions and other processes that consume additional electric charge.

3.3. Discharge characterization of batteries

Fig. 5 shows the discharge characteristics of the Zn–air battery at a constant current of 1 mA. From the observation, a flat polarization curve was observed at a potential around 1.35 V. The Zn–air battery demonstrated good specific capacity at about 460 mA h g^{-1}. This result is comparable with the theoretical specific capacity based on the molecular weight of ZnO (Linden, 2001). On the other hand, the discharge characteristic of the Zn–carbon battery at a constant current of 1 mA is shown in Fig. 6. A flat polarization curve was obtained at a high potential around 1.58 V. For the Zn–carbon battery, the system had a specific capacity of about 300 mA h g^{-1}.

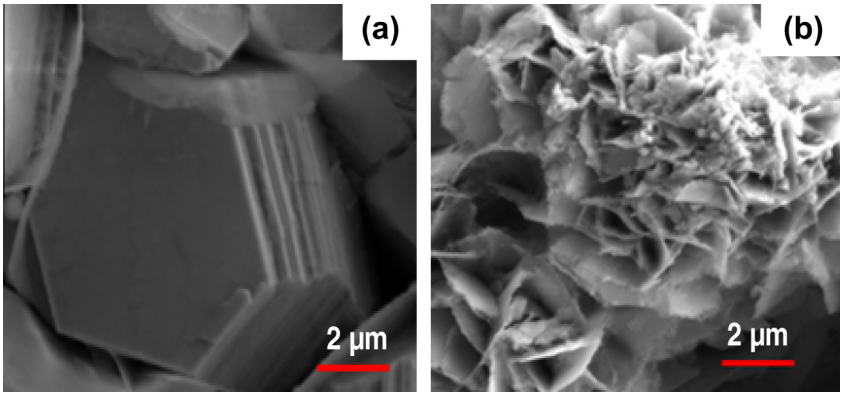

Figure 3 FESEM images of Zn electrodeposited at current densities of (a) 0.02 and (b) 0.10 A cm^{-2} at a higher magnification.

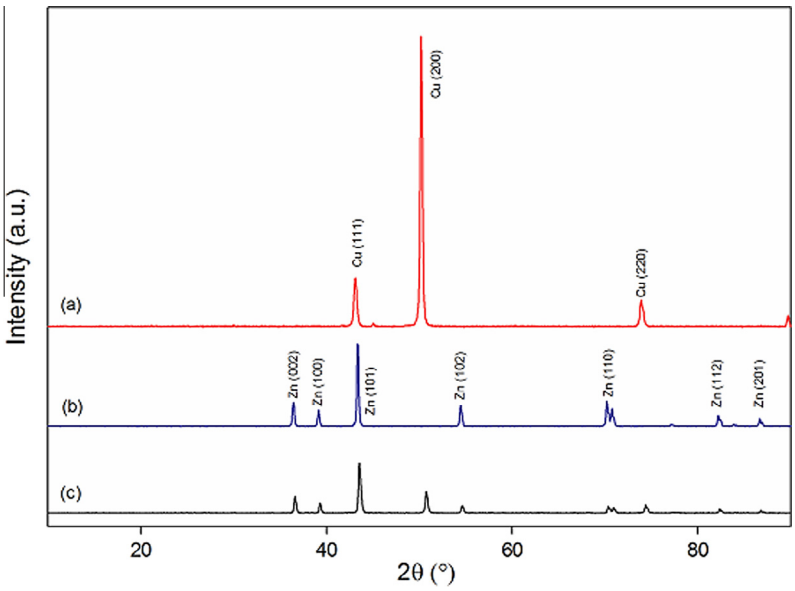

Figure 4 XRD pattern of (a) Cu plate, (b) Zn plate, and (c) Zn deposited at 0.02 A cm^{-2} for 1 h.

Table 1 Efficiency of Zn electrodeposition on the Cu plate at 0.02 A cm^{-2} for 1 h.

Sample	Mass gain (g)	Efficiency (%)
1	0.0276	95.17
2	0.0263	90.69
3	0.0277	95.52
4	0.0288	99.31

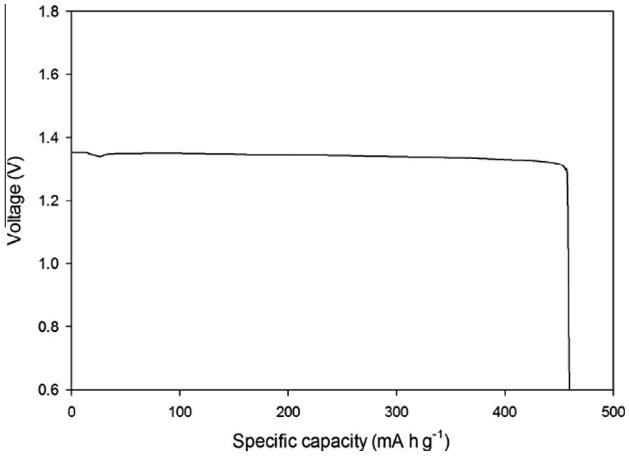

Figure 5 Discharge curve for the Zn–air battery at a constant discharge rate of 1 mA.

In fact, the amount of energy available from a battery is dependent on several aspects, which include the type of cell chemistry used, the amount of chemical material available in the cell, and the temperature of the operating cell. According to Linden (2001), the cathode material must be an efficient oxidizing agent, stable while in contact with the electrolyte, and possess useful working voltage. In the Zn–air battery system,

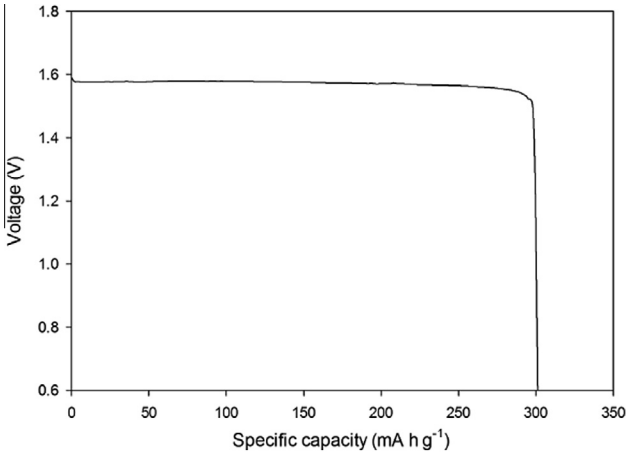

Figure 6 Discharge curve for the Zn–carbon battery at a constant discharge rate of 1 mA.

oxygen (O_2) was directly used from ambient air drawn into the cell. The overall electrochemical reactions of Zn–air batteries can be described as follows (Hamlen and Atwater, 2001):

$$Zn + 1/2O_2 + H_2O + 2(OH^-) \rightarrow Zn(OH)_4^{2-} \quad (5)$$

The initial discharge reaction at the Zn electrode is:

$$Zn + O^2 \rightarrow 2ZnO \quad (6)$$

For the Zn–carbon battery system, inert carbon was used to complete the electrical circuit. Eqs. (7)–(9) present the proposed chemical equation during the discharge process of the Zn–carbon battery.

$$\text{Anode}: \quad Zn \rightarrow Zn^{2+} + 2e^- \quad (7)$$

$$\text{Cathode}: \quad C + Zn^{2+} + 2e^- \rightarrow ZnC \quad (8)$$

$$\text{Overall}: \quad Zn + C \rightarrow ZnC \quad (9)$$

The Zn–air battery clearly had better performance with a high discharge capacity compared with the Zn–carbon battery even when similar Zn deposit samples were used as anode for both systems. This result is due to the fact that the Zn–air battery directly used oxygen from the atmosphere, which results in unlimited capacity and high energy density.

4. Conclusions

Zn was successfully deposited via the direct current electrodeposition process in $ZnSO_4$ solution without the presence of additives. Electrodeposition of pure Zn at a current density of 0.02 A cm^{-2} produced fine morphology with a high current efficiency without the presence of dendrites. Electrochemical results show that the Zn deposits achieved good specific capacity and stability during the discharge process for the Zn–air and Zn–carbon battery systems. Therefore, a good morphology of Zn deposits can be applied as anode materials in aqueous battery cells.

Acknowledgment

The authors would like to thank MN Masri for the experimental help and ERGS Grant No 203/PBAHAN/6730006 for the financial support in this study.

References

Abe, T. and Miyazaki, K., 2012, (Invited) Aqueous Electrolyte-Based Metal–Air Batteries: Challenges for Rechargeable Zinc Electrodes and Reversible Air Electrodes. Meeting Abstracts, 2012. The Electrochemical Society, p. 1182.

Baik, D.S., Fray, D.J., 2001. Electrodeposition of zinc from high acid zinc chloride solutions. J. Appl. Electrochem. 31, 1141–1147.

Bicelli, L.P., Bozzini, B., Mele, C., D'urzo, L., 2008. A review of nanostructural aspects of metal electrodeposition. Int. J. Electrochem. Sci. 3, 356–408.

Bunshah, R.F., 1994. Handbook of Deposition Technologies for Films and Coatings – Science, Second ed.. Technology and Applications William Andrew Publishing, Noyes.

Chu, M.G., Mcbreen, J., Adzic, G., 1981. Substrate effects on zinc deposition from zincate solutions. J. Electrochem. Soc. 128, 2281–2286.

Freitas, M.B.J.G., De Pietre, M.K., 2005. Deposit morphology of the zinc recovery by electrodeposition from the spent Zn–MnO_2 batteries. J. Power Sources 143, 270–274.

Gomes, A., Da Silva Pereira, M.I., 2006. Pulsed electrodeposition of Zn in the presence of surfactants. Electrochim. Acta 51, 1342–1350.

Hamlen, R.P., Atwater, T.B., 2001. Metal/Air Batteries Handbook of Batteries. D. Linden, T. B. Reddy, New York.

Hilder, M., Winther-Jensen, B., Clark, N.B., 2012. The effect of binder and electrolyte on the performance of thin zinc–air battery. Electrochim. Acta 69, 308–314.

Koh, J.C.H., Ahmad, Z.A., Mohamad, A.A., 2011. Self-aligned TiO_2 nanotube arrays produced by air–cathode as electrode. J. Alloys Compd. 509, 8707–8715.

Lehr, I.L., Saidman, S.B., 2012. Influence of sodium bis(2-ethylhexyl) sulfosuccinate (AOT) on zinc electrodeposition. Appl. Surf. Sci. 258, 4417–4423.

Leung, P.K., Ponce-De-Leon, C., Low, C.T.J., Walsh, F.C., 2011. Zinc deposition and dissolution in methanesulfonic acid onto a carbon composite electrode as the negative electrode reactions in a hybrid redox flow battery. Electrochim. Acta 56, 6536–6546.

Li, G.-R., Dawa, C.-R., Bu, Q., Lu, X.-H., Ke, Z.-H., Hong, H.-E., Zheng, F.-L., Yao, C.-Z., Liu, G.-K., Tong, Y.-X., 2007. Electrochemical self-assembly of ZnO nanoporous structures. J. Phys. Chem. C 111, 1919–1923.

Linden, D., 2001. Basic concepts. In: Linden, D., Reddy, T.B. (Eds.), Handbook of Batteries. McGraw Hill, New York.

Lou, H.H., Huang, Y., 2006. Electroplating. In Encyclopedia of Chemical Processing. Taylor & Francis.

Masri, M.N., Mohamad, A.A., 2009. Effect of adding potassium hydroxide to an agar binder for use as the anode in Zn–air batteries. Corrosion Sci. 51, 3025–3029.

Popov, K.I., Keca, D.N., Andelic, M.D., 1978. Electrodeposition of zinc on copper from alkaline zincate solutions. J. Appl. Electrochem., 19–23.

Shaigan, N., Qu, W., Takeda, T., 2010. Morphology Control of Electrodeposited Zinc from Alkaline Zincate Solutions for Rechargeable Zinc Air Batteries. J. Electrochem. Soc. 28, 35–44.

Sharifi, B., Mojtahedi, M., Goodarzi, M., Khaki, J.V., 2009. Effect of alkaline electrolysis conditions on current efficiency and morphology of zinc powder. Hydrometallurgy 99, 72–76.